International Journal of Information, Control and Computer Sciences
ISSN: 2517-9942
Vol:1, No:10, 2007

Control of Vibrations in Flexible Smart Structures using Fast Output Sampling Feedback Technique

T.C. Manjunath[1], *Student Member IEEE* , B. Bandyopadhyay, *IEEE member*

Abstract **—**This paper features the modeling and design of a Fast Output Sampling (FOS) Feedback control technique for the Active Vibration Control (AVC) of a smart flexible aluminium cantilever beam for a Single Input Single Output (SISO) case. Controllers are designed for the beam by bonding patches of piezoelectric layer as sensor / actuator to the master structure at different locations along the length of the beam by retaining the first 2 dominant vibratory modes. The entire structure is modeled in state space form using the concept of piezoelectric theory, Euler-Bernoulli beam theory, Finite Element Method (FEM) and the state space techniques by dividing the structure into 3, 4, 5 finite elements, thus giving rise to three types of systems, viz., system 1 (beam divided into 3 finite elements), system 2 (4 finite elements), system 3 (5 finite elements). The effect of placing the sensor / actuator at various locations along the length of the beam for all the 3 types of systems considered is observed and the conclusions are drawn for the best performance and for the smallest magnitude of the control input required to control the vibrations of the beam. Simulations are performed in MATLAB. The open loop responses, closed loop responses and the tip displacements with and without the controller are obtained and the performance of the proposed smart system is evaluated for vibration control.

Keywords**—**Smart structure, Finite element method, State space model, Euler-Bernoulli theory, SISO model, Fast output sampling, Vibration control, LMI

I. Introduction

VIBRATION control of any system is always a formidable challenge for any control system designer. Active control of vibrations [8], [22] relieves a designer from strengthening the structure from dynamic forces and the structure itself from extra weight and cost. The need for intelligent structures [3], such as smart structures arises from the high performance requirements of such structural members in numerous applications. Intelligent structures [3] are those which incorporate actuators and sensors that are highly integrated into the structure and have structural functionality, as well as highly integrated control logic, signal conditioning and power amplification electronics.

Considerable interest is focused on the modeling and control of smart structures with integrated piezoelectric layers. Culshaw [11] discussed the concept of smart structure, its benefits and applications. Baily and Hubbard [8] have studied the application of piezoelectric material as sensor / actuator for flexible structures. Hanagud *et.al.* [12] developed a Finite Element Model (FEM) for an active beam with many distributed piezoceramic sensors / actuators. Fanson *et.al.* [13] performed some experiments on a beam with piezoelectrics using positive position feedback. Balas [14] did extensive work on the feedback control of flexible piezoelectric structures. Experimental evaluation of piezoelectric actuation for the control of vibrations in a cantilever beam was presented by Burdess *et.al.* [19]. Yang and Lee [23] studied the optimization of feedback gain in control system design for structures. S.B. Choi *et.al.* presented a new technique of control of flexible structures by the use of distributed piezofilm sensors and actuators in [17]. Crawley [3] presented the development of piezoelectric sensor / actuator as elements of intelligent structures.

Feedback control of vibrations in mechanical flexible systems has numerous applications, like in aircrafts, active noise and shape control, acoustic control, control of space structures and in control of flexible manipulators. Active control of unwanted disturbance consists of canceling the disturbance by the deliberate addition of a second disturbance, equal in magnitude but opposite in direction. Applying forces whose magnitudes and phases are determined by a controller can control vibrations of single and multiple degree of freedom (DOF) systems. The inputs to the controller are displacements or velocities measured at various points in the system.

An active vibration control system consists of an actuator, controller, sensor and the system / plant (beam) which is to be controlled. Fully active actuators like Piezoelectrics, Magneto Rheological (MR) fluids, Piezoceramics, Electro-Rheological (ER) fluids, Shape Memory Alloys (SMA), PVDF can be used to generate a secondary vibrational response in a linear mechanical system. This could reduce the overall response of the system plant by destructive interference with the original response of the system, caused by the primary source of

[1] Mr. T.C. Manjunath is a Research Scholar, IEEE (No. 41561947) / ISSS / SPIE / IOP / SSI / ISOI / ISTE member, Interdisciplinary Programme in Systems and Control Engineering, Indian Institute of Technology Bombay, Powai, Mumbai-400076, Maharashtra, India. (Corresponding author phone : +91 22 25780263 / 25767884 ; Fax: +91 22 25720057 ; E-mail: tcmanju@sc.iitb.ac.in , tcmanjunath@rediffmail.com).

Dr. B. Bandyopadhyay is with the interdisciplinary programme in systems and control engineering, IIT Bombay, Mumbai-76, Maharashtra, India and is a Professor and Convener.

vibration [6].

Recent advances in smart structure technology provide a means for integrating sensors and actuators to the mechanical structure. Due to its fast response time, relatively good control force, low power consumption, high bandwidth, smart structures finds a lot of applications in vibration control of systems [10]. Numerous identification and control techniques have been proposed for active vibration suppression of flexible structures. Some of the various methods used for vibration control in systems are the periodic output feedback control [24], sliding mode control, fast output sampling feedback control [1], [2], [15] wave suppression method, independent modal space control method, modified independent modal space control method, higher order laminate beam theory and PID control. Control of vibrations (using the fast output sampling feedback control technique) in a flexible structure through smart structure concept for a SISO case is being *proposed* here in this paper.

In the present research work, a smart flexible cantilever beam is considered and the state space model is obtained using the FEM technique and using the Euler-Bernoulli theory. A new control algorithm is *proposed* to design a FOS feedback based controller for the flexible smart cantilever beam by bonding patches of piezoelectric layers as sensor / actuator pair to the master structure at different locations along the length of the beam as shown in Fig. 2. An external force input f_{ext} is applied at the free end of the beam for all the various models of the plant as shown in Fig. 2. There are two inputs to the plant. One is the external force input f_{ext}, which is taken as a load matrix of 1 unit in the simulation. The other input is the control input u to the actuator from the controller. Simulations are performed in Matlab. The actual response of the system, i.e., the tip displacement $w(x,t)$ is obtained for all the various models of the smart flexible system with and without the controllers by considering the first two dominant vibratory modes. In the work considered, both the tip displacement and the plot of time derivative of the displacement, i.e., the sensor output y as a function of time with the fast output sampling feedback gain **L** are observed.

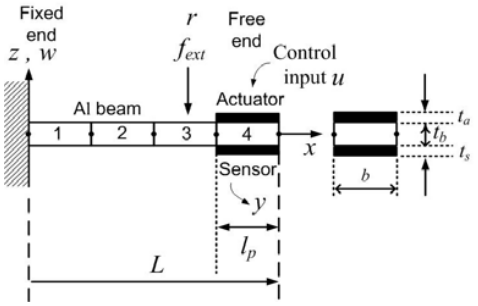

Fig. 1 A smart flexible beam made up of 4 finite elements with piezo patches as collocated pair at fixed end. 1, 2 and 3 are regular beam elements, 4 is a piezoelectric beam element

The paper is organized as follows. In Section 2, a state space model of the smart cantilever beam bonded with piezoelectric as sensor / actuator using the Finite Element Theory [7], [9], [16] is presented. Section 3 contains a brief review on the FOS control technique and the design of the FOS control technique [1], [2], [15] for the vibration control of the smart cantilever beam for different sensor / actuator locations for all the models of the 3 types of systems. The results and discussions are included in Section 4 followed by the simulation results and the references.

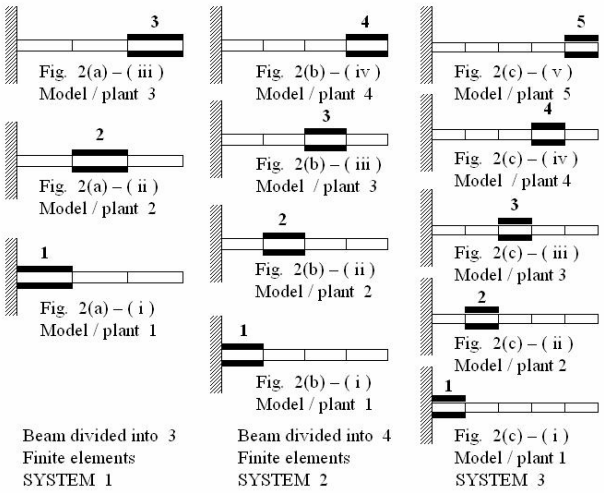

Fig. 2 A smart flexible Al cantilever beam divided into 3, 4, 5 finite elements, giving rise to 3 types of systems, viz., System 1(3 models), System 2 (4 models) and System 3 (5 models)

II. MODELING OF SMART STRUCTURES

The smart structure is modeled as follows.

A. Displacement functions

Consider a flexible cantilever beam element as shown in Fig. 3. The dimensions of the flexible cantilever beam is shown in Tables I. An external force input f_{ext} (impulse) is applied at the free end of the smart beam as shown in Fig. 4. The beam is subjected to vibrations. These vibrations are suppressed quickly in no time by the closed loop action of the controller, sensor and actuator. The free vibration characteristics of a flexible beam [25] is governed by the following fourth order differential equation

$$c^2 \frac{\partial^4 w(x,t)}{\partial x^4} + \frac{\partial^2 w(x,t)}{\partial x^2} = 0, \qquad (1)$$

where w is the transverse displacement of the beam and is a function x and t, x being the distance of the local coordinate from the fixed end, t being the time and c is a constant which is given by $\sqrt{EI/\rho A}$. E, I, ρ and A are the young's modulus, moment of inertia, mass density and area of the beam respectively. When a system vibrates as shown in the Fig. 3, it undergoes to and fro motion, it has transverse displacements and so all positions vary with time and therefore, the system has velocities and accelerations. Mass

times acceleration as inertia force appears in the governing differential equation of the beam which is given in (1), i.e., the equation of motion involves a fourth order derivative w.r.t. x and a second order derivative w.r.t. time (acceleration) The solution of the equation (1) is assumed as a cubic polynomial function of x given by

$$W(x) = a_1 + a_2 x + a_3 x^2 + a_4 x^3, \tag{2}$$

where the constants a_1 to a_4 are obtained by using the boundary conditions given below at both the nodal points (fixed end and free end) as

$$W(x) = w_1 \text{ and } \frac{\partial W}{\partial x} = u_1 = \theta_1; \text{ at } x = 0, \tag{3}$$

$$W(x) = w_2 \text{ and } \frac{\partial W}{\partial x} = u_2 = \theta_2; \text{ at } x = l_b, \tag{4}$$

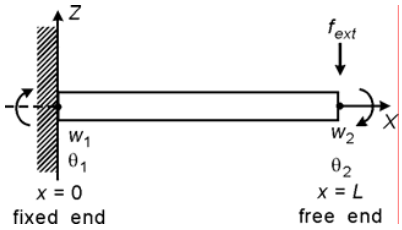

Fig. 3 Flexible cantilever beam element

TABLE I
PROPERTIES OF T HE FLEXIBLE CANTILEVER BEAM ELEMENT

Parameter (with units)	Symbol	Numerical values
Length (m)	l_b	0.075
Width (m)	b	0.03
Thickness (mm)	t_b	0.5
Young's modulus (Gpa)	E_b	193.06
Density (kg/m^3)	ρ_b	8030
Damping constants	$\alpha,\ \beta$	0.001. 0.0001

TABLE II
PROPERTIES OF T HE PIEZO - SENSOR / ACTUATOR ELEMENT

Parameter (with units)	Symbol	Numerical values
Length (m)	l_p	0.075
Width (m)	b	0.03
Thickness (mm)	t_a, t_s	0.35
Young's modulus (Gpa)	E_p	68
Density (kg/m^3)	ρ_p	7700
Piezo strain constant (m /V)	d_{31}	125×10^{-12}
Piezo stress constant (Vm / N)	g_{31}	10.5×10^{-3}

where w_1, u_1, θ_1 and w_2, u_2, θ_2 are the DOF's at the node 1 and node 2 respectively and l_b is the length of the regular beam element.

Application of the boundary condition given by equations (3) and (4) in (2) yields

$$\begin{bmatrix} a_1 \\ a_2 \\ a_3 \\ a_4 \end{bmatrix} = \frac{1}{l_b^3}\begin{bmatrix} l_b^3 & 0 & 0 & 0 \\ 0 & l_b^3 & 0 & 0 \\ -3l_b & -2l_b^2 & 3l_b & -l_b^2 \\ 2 & l_b & -2 & l_b \end{bmatrix}\begin{bmatrix} w_1 \\ \theta_1 \\ w_2 \\ \theta_2 \end{bmatrix}. \tag{5}$$

Substituting the constants obtained from (5) into (2) and by rearranging the terms, the final form for $W(x)$ is obtained as

$$[W(x)] = [\mathbf{n}]^T[\mathbf{q}]$$

$$= \begin{bmatrix} f_1(x) & f_2(x) & f_3(x) & f_4(x) \end{bmatrix}\begin{bmatrix} w_1 \\ \theta_1 \\ w_2 \\ \theta_2 \end{bmatrix}, \tag{6}$$

where $[\mathbf{n}]$ gives the shape functions as

$$[\mathbf{n}] = \begin{bmatrix} f_1(x) \\ f_2(x) \\ f_3(x) \\ f_4(x) \end{bmatrix} = \begin{bmatrix} 1 - 3\frac{x^2}{l_b^2} + 2\frac{x^3}{l_b^3} \\ x - 2\frac{x^2}{l_b} + 2\frac{x^3}{l_b^2} \\ 3\frac{x^2}{l_b^2} - 2\frac{x^3}{l_b^3} \\ -\frac{x^2}{l_b} + \frac{x^3}{l_b^2} \end{bmatrix} \tag{7}$$

and $[\mathbf{q}]$ is the vector of displacements and slopes (nodal displacement vector) and is given by

$$[\mathbf{q}] = \begin{bmatrix} w_1 \\ \theta_1 \\ w_2 \\ \theta_2 \end{bmatrix}. \tag{8}$$

The displacement, its first and second spatial derivatives and its time derivative is given by the equations

$$[W(x)] = [\mathbf{n}]^T[\mathbf{q}], \tag{9}$$

$$[W'(x)] = \frac{\partial W}{\partial x} = [\mathbf{n_2}]^T[\mathbf{q}],$$

$$= \begin{bmatrix} f_1'(x) & f_2'(x) & f_3'(x) & f_4'(x) \end{bmatrix}\begin{bmatrix} w_1 \\ \theta_1 \\ w_2 \\ \theta_2 \end{bmatrix}, \tag{10}$$

$$[W''(x)] = \frac{\partial^2 W}{\partial x^2} = [\mathbf{n_1}]^T[\mathbf{q}],$$

$$= \begin{bmatrix} f_1''(x) & f_2''(x) & f_3''(x) & f_4''(x) \end{bmatrix} \begin{bmatrix} w_1 \\ \theta_1 \\ w_2 \\ \theta_2 \end{bmatrix}, \quad (11)$$

$$[\dot{W}(x)] = \frac{\partial W}{\partial t} = [\mathbf{n_3}]^T[\dot{\mathbf{q}}],$$

$$= \begin{bmatrix} f_1(x) & f_2(x) & f_3(x) & f_4(x) \end{bmatrix} \begin{bmatrix} \dot{w}_1 \\ \dot{\theta}_1 \\ \dot{w}_2 \\ \dot{\theta}_2 \end{bmatrix}. \quad (12)$$

B. Dynamic equation of the beam element

The strain energy U and the kinetic energy T for the beam element with uniform cross section in bending is obtained as

$$U = \frac{E_b I_b}{2} \int_{l_b} \left[\frac{\partial^2 w}{\partial x^2} \right] dx,$$

$$= \frac{E_b I_b}{2} \int_{l_b} [w''(x,t)]^T [w''(x,t)] dx, \quad (13)$$

$$T = \frac{\rho_b A_b}{2} \int_{l_b} \left[\frac{\partial^2 w}{\partial t^2} \right] dt,$$

$$= \frac{\rho_b A_b}{2} \int_{l_b} [\dot{w}(x,t)]^T [\dot{w}(x,t)] dt, \quad (14)$$

where ρ_b is the mass density of the beam material, A_b is the cross sectional area of the beam, I_b is the moment of inertia of the beam and E_b is the modulus of elasticity of the beam material. The equation of motion of the regular beam element is obtained by the lagrangian equation

$$\frac{d}{dt}\left[\frac{\partial T}{\partial \dot{q}_i}\right] + \left[\frac{\partial U}{\partial q_i}\right] = [F_i] \quad (15)$$

as

$$M^b \ddot{q} + K^b q = f^b(t), \quad (16)$$

where M^b, K^b and f^b are the mass, stiffness and the force coefficient vectors of the regular beam element. The mass and stiffness matrices are obtained as

$$[M^b] = \rho_b A_b \int_{l_b} [\mathbf{n}_3]^T [\mathbf{n}_3] dx, \quad (17)$$

and

$$[K^b] = E_b I_b \int_{l_b} [\mathbf{n}_1]^T [\mathbf{n}_1] dx. \quad (18)$$

The resulting equation of motion for the regular beam element in its explicit form is obtained as

$$\frac{\rho_b A_b}{420} \begin{bmatrix} 156 & 22l_b & 54 & -13l_b \\ 22l_b & 4l_b^2 & 13l_b & -3l_b^2 \\ 54 & 13l_b & 156 & -22l_b \\ -13l_b & -3l_b^2 & -22l_b & 4l_b^2 \end{bmatrix} \begin{bmatrix} \ddot{w}_1 \\ \ddot{\theta}_1 \\ \ddot{w}_2 \\ \ddot{\theta}_2 \end{bmatrix} +$$

$$\frac{E_b I_b}{l_b} \begin{bmatrix} \frac{12}{l_b^2} & \frac{6}{l_b} & -\frac{12}{l_b^2} & \frac{6}{l_b} \\ \frac{6}{l_b} & 4 & -\frac{6}{l_b} & 2 \\ \frac{12}{l_b^2} & -\frac{6}{l_b} & \frac{12}{l_b^2} & -\frac{6}{l_b} \\ \frac{6}{l_b} & 2 & -\frac{6}{l_b} & 4 \end{bmatrix} \begin{bmatrix} w_1 \\ \theta_1 \\ w_2 \\ \theta_2 \end{bmatrix} = \begin{bmatrix} F_1 \\ M_1 \\ F_2 \\ M_2 \end{bmatrix}, \quad (19)$$

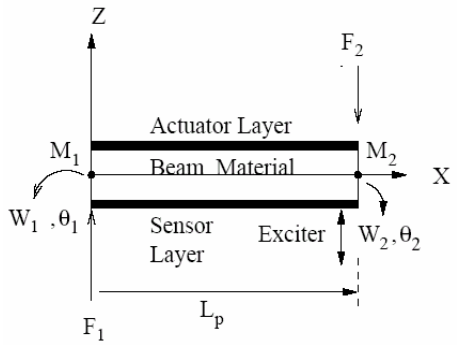

Fig. 4 Piezoelectric (PZT) beam element

where F_1 and F_2 are the forces at the nodes 1 and 2, M_1 and M_2 are the bending moments acting at the nodes 1 and 2 respectively. The piezoelectric beam element shown in Fig. 4 is obtained by sandwiching the regular beam element between two piezoelectric thin layers of thickness t_a or t_s. The dimensions of the piezoelectric patch are given in table II. The bottom layer acts as a sensor and the upper layer acts as an actuator. Similar to the equation (19) obtained for a regular beam element, the Lagrangian equation of motion of the piezoelectric beam element is obtained as

$$M^p \ddot{q} + K^p q = f^p(t), \quad (20)$$

where M^p and K^p are the mass and stiffness matrices of the piezoelectric element and is obtained as

$$[M^p] = \begin{bmatrix} 156 & 22l_b & 54 & -13l_b \\ 22l_b & 4l_b^2 & 13l_b & -3l_b^2 \\ 54 & 13l_b & 156 & -22l_b \\ -13l_b & -3l_b^2 & -22l_b & 4l_b^2 \end{bmatrix} \quad (21)$$

and

$$\left[K^{p}\right]=\frac{E\,I}{l_p}\begin{bmatrix}\frac{12}{l_p^2} & \frac{6}{l_p} & -\frac{12}{l_p^2} & \frac{6}{l_p}\\ \frac{6}{l_p} & 4 & -\frac{6}{l_p} & 2\\ \frac{12}{l_p^2} & -\frac{6}{l_p} & \frac{12}{l_p^2} & -\frac{6}{l_p}\\ \frac{6}{l_p} & 2 & -\frac{6}{l_p} & 4\end{bmatrix}. \quad (22)$$

Here,

$$E\,I = E_b I_b + 2\,E_p I_p\,, \quad (23)$$

$$I_p = \frac{1}{12}bt_a^3 + bt_a\left(\frac{t_a+t_b}{2}\right)^2, \quad (24)$$

and

$$\rho\,A = b\left(\rho_b t_b + 2\rho_p t_a\right). \quad (25)$$

C. Sensor equation

The sensor equation is derived from the direct piezoelectric equation. The electric displacement developed on the sensor surface is directly proportional to the stress acting on the sensor. If the poling is done along the thickness direction of the sensors with the electrodes on the upper and the lower surfaces, the electric displacement D is given by

$$D_z = d_{31} * E_p \varepsilon_x = e_{31}\varepsilon_x\,, \quad (26)$$

where d_{31} is the piezoelectric constant, e_{31} is the piezoelectric stress / charge constant, E_p is the young's modulus and ε_x is the strain that is produced.

The total charge $Q(t)$ developed on the sensor surface is the spatial summation of all the point charges developed on the sensor layer. Thus, the expression for the current generated is obtained as

$$i(t) = \frac{d\,Q(t)}{dt} = \frac{d}{dt}\int_A e_{31}\varepsilon_x\,dA = ze_{31}b\int_0^{l_p}\mathbf{n}_1^T\dot{\mathbf{q}}dx\,, \quad (27)$$

where $z = \frac{t_b}{2} + t_a$ and $\mathbf{n_1}$ given by (11).

This current is converted into the open circuit sensor voltage V^s using a signal-conditioning device with the gain G_c and applied to an actuator with the FOS controller having a gain $\mathbf{L}$. Thus, the sensor output voltage is obtained as

$$V^s(t) = G_c\,e_{31}\,z\,b\int_0^{l_p}\mathbf{n}_1^T\dot{\mathbf{q}}\,dx \quad (28)$$

which is nothing but the signal conditioning gain G_c multiplied by the closed circuit current $i(t)$ generated by the piezoelectric lamina. Substituting for $\mathbf{n}_1^T$ from (11) and $\dot{\mathbf{q}}$ from (12) and simplifying, we get the sensor voltage for a 2 node finite element as

$$V^s(t) = \begin{bmatrix}0 & -G_c\,e_{31}\,z\,b & 0 & G_c\,e_{31}\,z\,b\end{bmatrix}\begin{bmatrix}\dot{w}_1\\ \dot{\theta}_1\\ \dot{w}_2\\ \dot{\theta}_2\end{bmatrix} \quad (29)$$

$$V^s(t) = G_c\,e_{31}\,z\,b*\begin{bmatrix}0 & -1 & 0 & 1\end{bmatrix}\begin{bmatrix}\dot{w}_1\\ \dot{\theta}_1\\ \dot{w}_2\\ \dot{\theta}_2\end{bmatrix} \quad (30)$$

which can be further expressed as a scalar-vector product

$$V^s(t) = \mathbf{p}^T\dot{\mathbf{q}}\,, \quad (31)$$

where $\dot{\mathbf{q}}$ is the time derivative of the modal coordinate vector $\mathbf{q}$, $\mathbf{p}^T$ is a constant vector which depends on the type of sensor, its characteristics and its location on the beam. Note that the sensor output is a function of the second spatial derivative of the mode shape.

This sensor voltage is given as input to the controller and the output of the controller (which is nothing but the control input to the actuator, i.e., the actuator voltage) is the controller gain $\mathbf{L}$ multiplied by the sensor voltage $V^s(t)$. Thus, the input voltage to the actuator $V^a(t)$ is given by

$$V^a(t) = \mathbf{L}\,V^s(t) = \mathbf{L}\,G_c\,e_{31}\,z\,b\int_0^{l_p}\mathbf{n}_1^T\dot{\mathbf{q}}\,dx\,. \quad (32)$$

D. Actuator equation

The actuator strain is derived from the converse piezoelectric equation. The strain developed ε_a on the actuator layer is given by

$$\varepsilon_a = d_{31}E_f\,, \quad (33)$$

where d_{31} and E_f are the piezo strain constant and the electric field respectively. When the input to the piezoelectric actuator $V^a(t)$ is applied in the thickness direction t_a, the electric field, E_f which is the voltage applied $V^a(t)$ divided by the thickness of the actuator t_a; *and* the stress, σ_a which is the actuator strain multiplied by the young's modulus E_p of the piezo actuator layer are given by

$$E_f = \frac{V^a(t)}{t_a} \quad (34)$$

and

$$\sigma_a = E_p\,d_{31}\frac{V^a(t)}{t_a}. \quad (35)$$

The strain developed on the actuator layer is directly proportional to the electric field (E_f) and is given by

$$\varepsilon_a = d_{31} * E_f = d_{31} \frac{V^a(t)}{t_a}. \quad (36)$$

The resultant moment M_a acting on the beam is thus determined by integrating the stress through the structural thickness as

$$M_A = E_p\, d_{31}\, \bar{z}\, V^a(t), \quad (37)$$

where $\bar{z} = \frac{(t_a + t_b)}{2}$ is the distance between the neutral axis of the beam and the piezoelectric layer. Finally, the control force applied by the actuator is obtained as

$$f_{ctrl} = E_p\, d_{31}\, b\, \bar{z} \int_{l_p} \mathbf{n}_2\, dx\, V^a(t) \quad (38)$$

or can be expressed as a scalar vector product as

$$f_{ctrl} = \mathbf{h} V^a(t) = \mathbf{h} u(t), \quad (39)$$

where $\mathbf{n}_2{}^T$ is the first spatial derivative of the shape function of the flexible beam, $\mathbf{h}^T$ is a constant vector which depends on the type of actuator and its location on the beam, given by $\mathbf{h} = \begin{bmatrix} -E_p\, d_{31}\, b\, \bar{z} & 0 & E_p\, d_{31}\, b\, \bar{z} & 0 \end{bmatrix}$ and $u(t)$ is nothing but the control input to the actuator, i.e., $V^a(t)$ from the controller. If any external forces are acting on the beam, then the total force vector becomes

$$f^t = f_{ext} + f_{ctrl}. \quad (40)$$

E. Formulation

The dynamic equation of the smart structure is obtained by using both the regular and piezoelectric beam elements given by (17) - (22). The mass and stiffness of the bonding or the adhesive between the master structure and the sensor / actuator pair is neglected. The signal conditioning device gain (G_c) is assumed as 100. The cable capacitance between the sensor and signal-conditioning device is considered negligible and the temperature effects are neglected. The mass and stiffness of the entire beam, which is divided into 4 finite elements is assembled using the FEM technique [7], [9], [16] and the assembled matrices (global matrices), $\mathbf{M}$ and $\mathbf{K}$ are obtained.

The equation of motion of the smart structure is finally given by

$$\mathbf{M}\ddot{\mathbf{q}} + \mathbf{K}\mathbf{q} = f_{ext} + f_{ctrl} = f^t, \quad (41)$$

where $\mathbf{M}, \mathbf{K}, \mathbf{q}, f_{ext}, f_{ctrl}, f^t$ are the global mass matrix, global stiffness matrix of the smart beam, the vector of displacements and slopes, the external force applied to the beam, the controlling force from the actuator and the total force vector respectively.

The mass matrix $\mathbf{M}$, stiffness matrix $\mathbf{K}$ and the control force coefficient vector $\mathbf{h}^T$ in the system equation can be varied by changing the position of the piezo-patch and number of regular and piezoelectric beam elements.

The generalized coordinates are introduced into the (41) using a transformation $\mathbf{q} = \mathbf{T}\mathbf{g}$ in order to reduce it further such that the resultant equation represents the dynamics of the first two vibratory modes of the smart flexible cantilever beam.

$\mathbf{T}$ is the modal matrix containing the eigen vectors representing the first two vibratory modes. In the flexible system, the first two vibration modes ω_1 and ω_2 which are the most dominant modes compared to the other modes are being considered.

This method is used to derive the uncoupled equations governing the motion of the free vibrations of the system in terms of principal coordinates by introducing a linear transformation between the generalized coordinates $\mathbf{q}$ and the principal coordinates $\mathbf{g}$. The equation (41) now becomes

$$\mathbf{M}\mathbf{T}\ddot{\mathbf{g}} + \mathbf{K}\mathbf{T}\mathbf{g} = f_{ext} + f_{ctrl} = f^t. \quad (42)$$

Pre-multiplying (42) by $\mathbf{T}^T$, we get

$$\mathbf{T}^T\mathbf{M}\mathbf{T}\ddot{\mathbf{g}} + \mathbf{T}^T\mathbf{K}\mathbf{T}\mathbf{g} = \mathbf{T}^T f_{ext} + \mathbf{T}^T f_{ctrl} = \mathbf{T}^T f^t, \quad (43)$$

which can be rewritten as

$$\mathbf{M}^*\ddot{\mathbf{g}} + \mathbf{K}^*\mathbf{g} = \mathbf{f}^*_{ext} + \mathbf{f}^*_{ctrl} = \mathbf{f}^{t*}. \quad (44)$$

where the notations, $\mathbf{M}^*$, $\mathbf{K}^*$, $\mathbf{f}^*_{ext}$ and $\mathbf{f}^*_{ctrl}$ are given by $\mathbf{M}^* = \mathbf{T}^T\mathbf{M}\mathbf{T}$, $\mathbf{K}^* = \mathbf{T}^T\mathbf{K}\mathbf{T}$, $\mathbf{f}^*_{ext} = \mathbf{T}^T f_{ext}$ and $\mathbf{f}^*_{ctrl} = \mathbf{T}^T f_{ctrl}$ respectively.

The above equation (44) can be written as

$$\mathbf{M}^*\ddot{\mathbf{g}} + \mathbf{C}^*\dot{\mathbf{g}} + \mathbf{K}^*\mathbf{g} = \mathbf{f}^*_{ext} + \mathbf{f}^*_{ctrl} = \mathbf{f}^{t*} \quad (45)$$

by introducing the generalized structural modal damping matrix $\mathbf{C}^* = \alpha\mathbf{M}^* + \beta\mathbf{K}^*$, where α and β are the frictional damping constant and the structural damping constant used in $\mathbf{C}^*$.

Here, $\mathbf{M}^*$, $\mathbf{K}^*$, $\mathbf{f}^*_{ext}$ and $\mathbf{f}^*_{ctrl}$ represents the generalized mass matrix, the generalized stiffness matrix, the generalized external force vector and the generalized control force vector respectively. The governing equation (45) decouples into the equations corresponding to each individual mode.

The generalized external force coefficient vector is

$$\mathbf{f}^*_{ext} = \mathbf{T}^T \mathbf{f}_{ext} = \mathbf{T}^T f\, r(t), \quad (46)$$

where $r(t)$ is the external force input (impulse disturbance) to the beam.

The generalized control force coefficient vector is

$$\mathbf{f}^*_{ctrl} = \mathbf{T}^T f_{ctrl} = \mathbf{T}^T\mathbf{h} V^a(t) = \mathbf{T}^T\mathbf{h}\, u(t). \quad (47)$$

F. State space model of the smart cantilever beam

The governing equation (45) can be written in state space form as follows. Let the states of the system be defined as

$$\mathbf{g} = x,$$
$$\mathbf{g} = \begin{bmatrix} g_1 \\ g_2 \end{bmatrix} = \begin{bmatrix} x_1 \\ x_2 \end{bmatrix} = x, \tag{48}$$

and

$$\dot{\mathbf{g}} = \dot{x} = \begin{bmatrix} \dot{x}_1 \\ \dot{x}_2 \end{bmatrix} = \begin{bmatrix} x_3 \\ x_4 \end{bmatrix} \text{ and } \ddot{\mathbf{g}} = \begin{bmatrix} \dot{x}_3 \\ \dot{x}_4 \end{bmatrix}. \tag{49}$$

Using (46) to (49) in (45) becomes

$$\mathbf{M}^* \begin{bmatrix} \dot{x}_3 \\ \dot{x}_4 \end{bmatrix} + \mathbf{C}^* \begin{bmatrix} x_3 \\ x_4 \end{bmatrix} + \mathbf{K}^* \begin{bmatrix} x_1 \\ x_2 \end{bmatrix} = \mathbf{f}_{ext}^* + \mathbf{f}_{ctrl}^*. \tag{50}$$

which can be further simplified as

$$\begin{bmatrix} \dot{x}_3 \\ \dot{x}_4 \end{bmatrix} = -\mathbf{M}^{*-1}\mathbf{K}^* \begin{bmatrix} x_1 \\ x_2 \end{bmatrix} - \mathbf{M}^{*-1}\mathbf{C}^* \begin{bmatrix} x_3 \\ x_4 \end{bmatrix} + \mathbf{M}^{*-1}\mathbf{f}_{ext}^* + \mathbf{M}^{*-1}\mathbf{f}_{ctrl}^*. \tag{51}$$

and finally written in state equation form as

$$\begin{bmatrix} \dot{x}_1 \\ \dot{x}_2 \\ \dot{x}_3 \\ \dot{x}_4 \end{bmatrix} = \begin{bmatrix} 0 & I \\ -\mathbf{M}^{*-1}\mathbf{K}^* & -\mathbf{M}^{*-1}\mathbf{C}^* \end{bmatrix} \begin{bmatrix} x_1 \\ x_2 \\ x_3 \\ x_4 \end{bmatrix} + \begin{bmatrix} 0 \\ \mathbf{M}^{*-1}\mathbf{T}^T\mathbf{h} \end{bmatrix} \mathbf{u}(t) + \begin{bmatrix} 0 \\ \mathbf{M}^{*-1}\mathbf{T}^T\mathbf{f} \end{bmatrix} r(t), \tag{52}$$

i.e.,

$$\dot{\mathbf{X}} = \mathbf{A}\,x(t) + \mathbf{B}\,u(t) + \mathbf{E}\,r(t) \tag{53}$$

The output equation (sensor equation) for a SISO case is given by

$$y(t) = V^s(t) = \mathbf{p}^T\dot{\mathbf{q}} = \mathbf{p}^T\mathbf{T}\dot{\mathbf{g}} = \mathbf{p}^T\mathbf{T}\begin{bmatrix} x_3 \\ x_4 \end{bmatrix}, = \begin{bmatrix} 0 & \mathbf{p}^T\mathbf{T} \end{bmatrix} \begin{bmatrix} x_1 \\ x_2 \\ x_3 \\ x_4 \end{bmatrix}, \tag{54}$$

and written in output equation form as

$$y(t) = \mathbf{C}^T\,x(t) + \mathbf{D}\,u(t). \tag{55}$$

The SISO state space model (state equation and output equation) of the smart flexible cantilever beam finally is given by

$$\dot{\mathbf{X}} = \mathbf{A}\,x(t) + \mathbf{B}\,u(t) + \mathbf{E}\,r(t), \quad y(t) = \mathbf{C}\,x(t) + \mathbf{D}\,u(t), \tag{56}$$

with

$$\mathbf{A} = \begin{bmatrix} 0 & I \\ -\mathbf{M}^{*-1}\mathbf{K}^* & -\mathbf{M}^{*-1}\mathbf{C}^* \end{bmatrix}_{(4\times 4)}, \mathbf{B} = \begin{bmatrix} \mathbf{0} \\ \mathbf{M}^{*-1}\mathbf{T}^T\mathbf{h} \end{bmatrix}_{(4\times 1)},$$

$$\mathbf{C}^T = \begin{bmatrix} \mathbf{0} & \mathbf{p}^T\mathbf{T} \end{bmatrix}_{(1\times 4)}, \ \mathbf{D} = 0 \ ; \ \mathbf{E} = \begin{bmatrix} 0 \\ \mathbf{M}^{*-1}\mathbf{T}^T\mathbf{f} \end{bmatrix}_{(4\times 1)}.$$

The smart flexible cantilever beam as shown in Fig. 3 is divided into a number of finite elements as shown in Fig. 2, viz., three (system 1-Fig. 2(a)), four (system 2-Fig. 2(b)) and five (system 3-Fig. 2(c)). The piezoelectric sensor / actuator is bonded to the smart structure at finite elements from free end to the fixed end. The state space model in (56) is obtained for various sensor / actuator locations on the cantilever beam by using

- 2 regular beam elements and 1 piezo electric element as shown in Fig. 2(a) - 3 models of system 1.
- 3 regular beam elements and 1 piezo electric element as shown in Fig. 2(b) - 4 models of system 2.
- 4 regular beam elements and 1 piezo electric element as shown in Fig. 2(c) - 5 models of system 3.

By placing a piezoelectric element as sensor / actuator at one finite element of the cantilever beam and making other elements as regular beam elements as shown in Figs. 2(a)-(c) and by varying the position of the piezoelectric sensor / actuator from the free end to the fixed end, various state space models are obtained. Then, the control of these models is obtained using the FOS feedback control technique, which is considered, in the next section.

Consider the 3 systems shown in Fig. 2(a)-(i), 2(b)-(i), 2(c)-(i). State space models of the smart cantilever beam with sensor / actuator pair at element 1 (fixed end) is represented by (56) with

$$\mathbf{A_{11}} = 10^4\begin{bmatrix} 0 & 0 & 0.0001 & 0 \\ 0 & 0 & 0 & 0.0001 \\ -5.0976 & -0.0000 & -0.0005 & -0.0000 \\ -0.0000 & -0.2266 & -0.0000 & -0.0000 \end{bmatrix};$$
$$\mathbf{B_{11}} = \begin{bmatrix} 0 \\ 0 \\ -0.1175 \\ -0.0093 \end{bmatrix}; \mathbf{E_{11}} = 10^2\begin{bmatrix} 0 \\ 0 \\ -2.2114 \\ -1.0906 \end{bmatrix}; \tag{57}$$
$$\mathbf{C_{11}}^T = \begin{bmatrix} 0 & 0 & -0.0050 & -0.0028 \end{bmatrix},$$

$$\mathbf{A_{12}} = 10^4\begin{bmatrix} 0 & 0 & 0.0001 & 0 \\ 0 & 0 & 0 & 0.0001 \\ -5.2872 & -0.0000 & -0.0005 & -0.0000 \\ -0.0000 & -0.1752 & -0.0000 & -0.0000 \end{bmatrix};$$
$$\mathbf{B_{12}} = \begin{bmatrix} 0 \\ 0 \\ -0.0791 \\ -0.0046 \end{bmatrix}; \mathbf{E_{12}} = 10^2\begin{bmatrix} 0 \\ 0 \\ -2.7116 \\ -1.1669 \end{bmatrix}; \tag{58}$$
$$\mathbf{C_{12}}^T = \begin{bmatrix} 0 & 0 & 0.0038 & -0.0016 \end{bmatrix},$$
$$\mathbf{D_{12}} = \textit{Null matrix},$$

$$\mathbf{A}_{13}=10^4\begin{bmatrix}0 & 0 & 0.0001 & 0\\ 0 & 0 & 0 & 0.0001\\ -5.0516 & 0.0000 & -0.0005 & 0.0000\\ 0.0000 & -0.1488 & 0.0000 & -0.0000\end{bmatrix};$$

$$\mathbf{B}_{13}=\begin{bmatrix}0\\0\\0.0514\\-0.0027\end{bmatrix};\mathbf{E}_{13}=10^3\begin{bmatrix}0\\0\\-3.0567\\-1.2241\end{bmatrix};\qquad(59)$$

$$\mathbf{C}_{13}{}^T=\begin{bmatrix}0 & 0 & 0.0026 & -0.0010\end{bmatrix}.$$

TABLE III
CHARACTERISTICS OF THE SMART BEAM IN FIG. 2 (a) WITH BEAM DIVIDED INTO 3 FINITE ELEMENTS (SYSTEM 1).

Position of sensor / actuator	Eigen values	Natural Freq. (Hz)
Element 1 : Fixed end	–2.55 ± *j* 225.76	35.93
(Model 1)	–0.11 ± *j* 47.61	7.57
Element 2 : Middle end	–2.1 ± *j* 204.69	32.57
(Model 2)	–0.04 ± *j* 26.44	4.21
Element 3 : Free end	–1.32 ± *j* 162.58	27.87
(Model 3)	–0.02 ± *j* 19.16	3.04

TABLE IV
CHARACTERISTICS OF THE SMART BEAM IN FIG. 2 (b) WITH BEAM DIVIDED INTO 4 FINITE ELEMENTS (SYSTEM 2).

Position of sensor / actuator	Eigen values	Natural Freq. (Hz)
Element 1 : Fixed end	–2.64 ± *j* 229.92	36.89
(Model 1)	–0.09 ± *j* 41.86	6.66
Element 2	–1.19 ± *j* 172.35	27.43
(Model 2)	–0.04 ± *j* 29.77	4.73
Element 3	–1.84 ± *j* 191.81	30.52
(Model 3)	–0.03 ± *j* 24.22	3.85
Element 4 : Free end	–1.27 ± *j* 159.23	25.34
(Model 4)	–0.02 ± *j* 19.89	3.16

TABLE V
CHARACTERISTICS OF THE SMART BEAM IN FIG. 2 (c) WITH BEAM DIVIDED INTO 5 FINITE ELEMENTS (SYSTEM 3).

Position of sensor / actuator	Eigen values	Natural Freq. (Hz)
Element 1 : Fixed end	–2.53 ± *j* 224.74	35.76
(Model 1)	–0.07 ± *j* 38.57	6.14
Element 2	–1.34 ± *j* 163.70	26.05
(Model 2)	–0.05 ± *j* 31.06	4.94
Element 3 : Middle end	–1.65 ± *j* 181.19	28.88
(Model 3)	–0.04 ± *j* 26.90	4.28
Element 4	–1.69 ± *j* 183.93	29.27
(Model 4)	–0.03 ± *j* 26.63	3.76
Element 5 : Free end	–1.24 ± *j* 157.68	25.09
(Model 5)	–0.02 ± *j* 20.57	3.27

The state space models of the smart cantilever beam divided into 3 finite elements with sensor / actuator pair at element 2, 3 (free end), 4 finite elements with sensor / actuator pair at elements 2, 3, 4 (free end), 5 finite elements with sensor / actuator pair at elements 2,3,4,5 (free end) are obtained similarly. The characteristics of the smart cantilever beam with the piezo pair at various locations along the length of the beam for different models of the three systems in Fig. 2 are given in Tables III - V.

III. CONTROL OF THE SMART STRUCTURE

In the following section, we develop the control strategy for the SISO representation of the developed smart structure model using the fast output sampling feedback control law [1], [2], [15] with 1 actuator input u and 1 sensor output y to control the vibrations of the flexible beam. In this type of control law as shown in Fig. 5, the value of the input at a particular moment depends on the output value at a time prior to this moment (namely at the beginning of the period).

Werner and Furuta [1], [2], [15] have shown that the poles of the discrete time control system could be assigned arbitrarily (within the natural restriction that they should be located symmetrically with respect to the real axis) using the fast output sampling technique. Since the feedback gains are piecewise constants [20], [21] their method could easily be implemented, guarantees the closed loop stability and indicated a new possibility. Such a control law can stabilize a much larger class of systems.

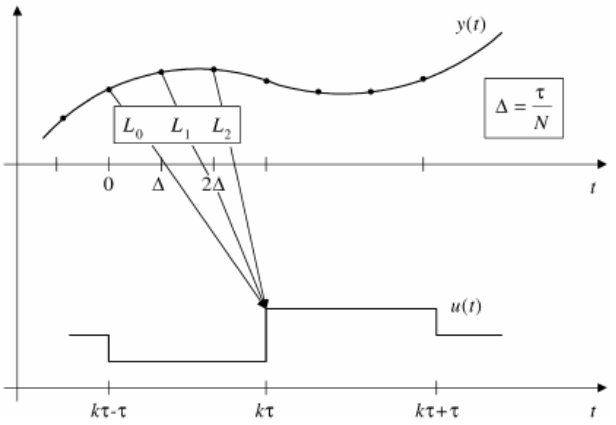

Fig. 5 Graphical illustration of fast output sampling feedback method

Consider a plant described by a LTI state space model given by

$$\dot{x}(t)=\mathbf{A}x(t)+\mathbf{B}u(t),\quad y(t)=\mathbf{C}x(t),\qquad(60)$$

where $x\in\Re^n$, $u\in\Re^m$, $y\in\Re^p$, $\mathbf{A}\in\Re^{n\times n}$, $\mathbf{B}\in\Re^{n\times m}$, $\mathbf{C}\in\Re^{p\times n}$, $\mathbf{A},\mathbf{B},\mathbf{C}$, are constant matrices of appropriate dimensions and it is assumed that the model is controllable and observable. Assume that output measurements are available at time instants $t=k\tau$, where $k=0,1,2,3,....$ Now, construct a discrete LTI system from these output

measurements at sampling rate $\frac{1}{\tau}$ (sampling interval of τ secs) during which the control signal u is held constant. The system obtained so is called as the τ system and is given by

$$\begin{aligned} x((k+1)\tau) &= \Phi_\tau x(k\tau) + \Gamma_\tau u(k\tau), \\ y(k\tau) &= \mathbf{C}\, x(k\tau), \end{aligned} \tag{61}$$

where $\Phi_\tau, \Gamma_\tau, \mathbf{C}$ are constant matrices of appropriate dimensions.

Assume that plant is to be controlled by a digital computer, with sampling interval τ and zero order hold and that a sampled data state feedback design has been carried out to find a state feedback gain F such that closed loop system

$$x(k\tau+\tau) = (\Phi_\tau + \Gamma_\tau F)x(k\tau) \tag{62}$$

has desirable properties.

Let $\Delta = \frac{\tau}{N}$, where $N >$ the observability index υ of the system. The control signal $u(k)$, which is applied during the interval $k\tau \le t \le (k+1)\tau$ is then generated according to

$$\begin{aligned} u(k) &= \begin{bmatrix} L_0 & L_1 & \ldots\ldots & L_{N-1} \end{bmatrix} \begin{bmatrix} y(k\tau-\tau) \\ y(k\tau-\tau+\Delta) \\ \vdots \\ \vdots \\ y(k\tau-\Delta) \end{bmatrix}, \\ &= \mathbf{L}\, y_k \end{aligned} \tag{63}$$

where the matrix blocks L_j represent the output feedback gains and the notations $\mathbf{L}$, y_k has been introduced here for convenience. Note that $\frac{1}{\tau}$ is the rate at which the loop is closed, whereas the output samples are taken at the N - times faster rate $\frac{1}{\Delta}$. To show how a FOS controller in (63) can be designed to realize the given sampled data state feedback gain for a controllable and observable system, we construct a fictitious, lifted system for which (63) can be interpreted as static output feedback [4], [18]. Let $(\Phi, \Gamma, \mathbf{C})$ denote the system (Δ system) in (60) sampled at the rate $\frac{1}{\Delta}$.

Consider the discrete time system having at time $t = k\tau$, the input $u_k = u(k\tau)$, the state $x_k = x(k\tau)$ and the output y_k as

$$\begin{aligned} x_{k+1} &= \Phi_\tau x_k + \Gamma_\tau u_k, \\ y_{k+1} &= \mathbf{C}_0 x_k + \mathbf{D}_0 u_k, \end{aligned} \tag{64}$$

where

$$\mathbf{C}_0 = \begin{bmatrix} \mathbf{C} \\ \mathbf{C}\Phi \\ \vdots \\ \mathbf{C}\Phi^{N-1} \end{bmatrix}; \quad \mathbf{D}_0 = \begin{bmatrix} 0 \\ \mathbf{C}\Gamma \\ \vdots \\ \mathbf{C}\sum_{j=0}^{N-2} \Phi^j \Gamma \end{bmatrix}. \tag{65}$$

Now, design a state feedback gain F such that $(\Phi_\tau + \Gamma_\tau F)$ has no eigen values at the origin and provides the desired closed loop behavior. Then, assuming that in the interval $k\tau \le t \le (k\tau + \tau)$,

$$u(t) = F\, x(k\tau), \tag{66}$$

one can define the fictitious measurement matrix,

$$\mathbf{C}(F, N) = (\mathbf{C}_0 + \mathbf{D}_0 F)(\Phi_\tau + \Gamma_\tau F)^{-1}, \tag{67}$$

which satisfies the fictitious measurement equation

$$y_k = \mathbf{C}\, x_k. \tag{68}$$

For $\mathbf{L}$ to realize the effect of F, it must satisfy the equation.

$$\mathbf{LC} = F. \tag{69}$$

Let υ denote the observability index of $(\Phi, \Gamma, \mathbf{C})$. It can be shown that for $N \ge \upsilon$, generically $\mathbf{C}$ has full column rank, so that any state feedback gain can be realized by a fast output sampling gain $\mathbf{L}$. If the initial state is unknown, there will be an error $\Delta u_k = u_k - F x_k$ in constructing the control signal under the state feedback; one can verify that the closed-loop dynamics are governed by

$$\begin{bmatrix} x_{k+1} \\ \Delta u_{k+1} \end{bmatrix} = \begin{bmatrix} \Phi_\tau + \Gamma_\tau F & \Gamma_\tau \\ 0 & \mathbf{L}\mathbf{D}_0 - F\Gamma_\tau \end{bmatrix} \begin{bmatrix} x_k \\ \Delta u_k \end{bmatrix}. \tag{70}$$

The system in (64) is stable if F stabilizes and only if (Φ_τ, Γ_τ) and the matrix $(\mathbf{L}\mathbf{D}_0 - F\Gamma_\tau)$ has all its Eigen values inside the unit circle. Thus, one can say that the eigen-values of the closed-loop system under a fast output sampling control law given in (63) are those of $(\Phi_\tau + \Gamma_\tau F)$ together with those of $(\mathbf{L}\mathbf{D}_0 - F\Gamma_\tau)$. This suggests that the state feedback F should be obtained so as to ensure the stability of both $(\Phi_\tau + \Gamma_\tau F)$ and $(\mathbf{L}\mathbf{D}_0 - F\Gamma_\tau)$.

The problem with controllers obtained in this way is that, although they are stabilizing and achieve the desired closed loop behavior in the output sampling instants, they may cause an excessive oscillation between sampling instants. The FOS feedback gains obtained may be very high. To reduce this effect, we relax the condition that $\mathbf{L}$ exactly satisfy the linear equation (69) and include a constraint on the gain $\mathbf{L}$. Thus, we arrive at the following equations as

$$\begin{aligned} \|L\| &< \rho_1; \\ \|\mathbf{L}\mathbf{D}_0 - F\Gamma_\tau\| &< \rho_2; \\ \|\mathbf{L}\mathbf{C} - F\| &< \rho_3. \end{aligned} \tag{71}$$

This can be formulated in the form of Linear Matrix Inequalities (LMI) [5] as

$$\begin{bmatrix} -\rho_1^{\,2} I & \mathbf{L} \\ \mathbf{L}^T & -I \end{bmatrix} < 0 \; ;$$
$$\begin{bmatrix} -\rho_2^{\,2} I & \mathbf{L}\mathbf{D}_0 - F\Gamma_\tau \\ (\mathbf{L}\mathbf{D}_0 - F\Gamma_\tau)^T & -I \end{bmatrix} < 0 \; ; \quad (72)$$
$$\begin{bmatrix} -\rho_3^{\,2} I & \mathbf{L}\mathbf{C} - F \\ (\mathbf{L}\mathbf{C} - F)^T & -I \end{bmatrix} < 0$$

ρ_1, ρ_2, ρ_3 represent the upper bounds on the spectral norms of $\mathbf{L}$, $\mathbf{L}\mathbf{D}_0 - F\Gamma_\tau$ and $\mathbf{L}\mathbf{C} - F$ respectively. These 3 objectives have been expressed by the upper bounds on matrix norms and each should be as small as possible. ρ_1 means low noise sensitivity, ρ_2 small means fast decay of observation error and most importantly, ρ_3 small means that fast output sampling controller with gain $\mathbf{L}$ is a good approximation of the originally designed state feedback controller. In this form, the LMI control optimization tool box for Matlab can be used to minimize a linear combination of ρ_1, ρ_2, ρ_3 and for the synthesis of $\mathbf{L}$ [5]. The following approach turned out to be useful. The fast output sampling feedback controller obtained by the above method requires only constant gains and hence is easier to implement.

The FOS control technique discussed above is used to design a controller to suppress the 1st 2 vibration modes of a smart flexible cantilever beam through smart structure concept for the various models of the 3 types of systems shown in Fig. 2. Controllers are designed for the various models of the smart structure system using the developed state space models for the sensor / actuator locations at various positions along the length of the beam for the various models of the 3 systems as given in (56) and its performance is evaluated for vibration control.

The first task in designing the FOS controller is the selection of the sampling interval τ. The maximum bandwidth for all the sensor / actuator locations on the beam are calculated (here, the 2nd vibratory mode of the plant) and then by using existing empirical rules for selecting the sampling interval based on bandwidth, approximately 10 times of the maximum 2nd vibration mode frequency of the system has been selected. The sampling interval used is $\tau = 0.004$ seconds. The number of sub-intervals N is chosen as 4. Simulations are carried out in Matlab.

Let $(\Phi_\tau, \Gamma_\tau, \mathrm{C})$ be the discrete time systems (tau system) of the systems in Fig. 2 in (56) sampled at a rate of $1/\tau$ seconds respectively and are given by

$$\Phi_{\tau 11} = \begin{bmatrix} 0.6217 & -0.0000 & 0.0034 & -0.0000 \\ -0.0000 & 0.9819 & -0.0000 & 0.0040 \\ -175.4999 & -0.0000 & -0.6042 & -0.0000 \\ -0.0000 & -9.0062 & -0.0000 & -0.9810 \end{bmatrix},$$
$$\Gamma_{\tau 11} = 1e^{-3} \begin{bmatrix} 0 \\ 0 \\ -0.1175 \\ -0.0093 \end{bmatrix} \quad (73)$$

for the model shown in the Fig. 2(a)-(i),

$$\Phi_{\tau 12} = \begin{bmatrix} 0.6087 & -0.0000 & 0.0034 & -0.0000 \\ -0.0000 & 0.9860 & -0.0000 & -0.0040 \\ -180.9848 & -0.0000 & 0.5906 & -0.0000 \\ -0.0000 & -6.9747 & -0.0000 & -0.9853 \end{bmatrix};$$
$$\Gamma_{\tau 12} = 1e^{-3} \begin{bmatrix} -0.0006 \\ -0.0000 \\ -0.2707 \\ -0.0182 \end{bmatrix} \quad (74)$$

for the model shown in the Fig. 2(b)-(i) and

$$\Phi_{\tau 13} = \begin{bmatrix} 0.6249 & 0.0000 & 0.0034 & 0.0000 \\ 0.0000 & 0.9881 & 0.0000 & 0.0040 \\ -174.1562 & 0.0000 & 0.6074 & 0.0000 \\ 0.0000 & -5.9265 & 0.0000 & 0.9875 \end{bmatrix},$$
$$\Gamma_{\tau 13} = 1e^{-3} \begin{bmatrix} -0.0004 \\ -0.0000 \\ -0.1771 \\ -0.0108 \end{bmatrix} \quad (75)$$

for the model shown in the 2(c)-(i). It is found that the tau systems are controllable and observable. The ranks of the matrices are 4. Similarly, the tau systems for other models of the 3 systems are obtained.

The stabilizing state feedback gains are obtained for each of the tau systems such that the eigenvalues of $(\Phi_\tau + \Gamma_\tau F)$ lie inside the unit circle and the response of the system has a good settling time. The impulse response of the system with the state feedback gain F is obtained.

Let $(\Phi, \Gamma, \mathrm{C})$ be the discrete time systems (delta system) of the system in Fig. 2 in (56) sampled at the rate $1/\Delta$ secs respectively, where $\Delta = \tau / N$. The delta systems for all the models of the 3 systems are obtained. Finally, the fast output sampling feedback gain $\mathbf{L}$ for any model of the system is obtained by solving $\mathbf{L}\mathbf{C} = F$ using the LMI optimization method [5] and is given by

$$\mathbf{L}_{11} = [\,78.52 \quad 54.16 \quad -83.75 \quad -72.33\,],$$
$$\mathbf{L}_{12} = [\,66.60 \quad -54.21 \quad -62.36 \quad 61.26\,], \quad (76)$$
$$\mathbf{L}_{13} = [\,-26.66 \quad 24.25 \quad -13.91 \quad 11.51\,],$$

for the models 1 of system 1, 2 and 3 and

$$\mathbf{L}_{31} = [\,116.52 \quad 124.16 \quad -83.75 \quad -32.33\,],$$
$$\mathbf{L}_{42} = [\,56.60 \quad 74.21 \quad -82.36 \quad 69.26\,], \qquad (77)$$
$$\mathbf{L}_{53} = [\,36.66 \quad -24.25 \quad -83.91 \quad 93.51\,].$$

for the models 3, 4 and 5 of the systems 1, 2 and 3 respectively.

The closed loop impulse responses (sensor outputs) with FOS feedback gain $\mathbf{L}$, the tip displacements and the plot of control effort u as a function of time t are obtained for the state space models of the system shown in the Fig. 2(a)-(i), 2(b)-(i), 2(c)-(i) respectively. The various responses are observed for the different models of the 3 systems similarly. Here in this paper, only the responses at the fixed end and the free ends of the 3 systems are shown for convenience. The results are compared and the conclusions are drawn for the best performance.

IV. Conclusion

Controllers have been designed for the smart flexible cantilever beam using the FOS feedback control technique for the three systems to suppress the 1st 2 vibratory modes. The flexible cantilever beam was divided into 3 elements (system 1), 4 elements (system 2) and 5 elements (system 3) and the sensor / actuator pairs were bonded to the structure at various finite elements, thus giving rise to various models of the 3 systems. Various state space models were obtained. The various responses are obtained for each of the models for the three systems. Here, the comparison and discussion of the simulation results of the vibration control for the smallest magnitude of the control effort u required to control the vibrations of the smart cantilever beam is presented.

From the simulation results, it is observed that modeling a smart structure by including the sensor / actuator mass and stiffness and by varying its location on the beam from the free end to the fixed end introduces a considerable change in the system's structural vibration characteristics. From the responses of the various models of each system, it is observed that when the piezoelectric element is placed near the clamped end, i.e., the fixed end, the sensor output voltage is greater.

This is due to the heavy distribution of the bending moment near the fixed end for the fundamental mode, thus leading to a larger strain rate. The sensor voltage is very less when the sensor / actuator pair is located at the free end. The sensitivity of the sensor / actuator pair depends on its location on the beam. From the output responses shown in the Figs. 6 - 11, it is observed that the control effort u required from the controller gets reduced if the sensor / actuator placement location is moved towards the fixed end.

A small magnitude of the control signal u is sufficient to control the structural vibrations of each model of the systems 1, 2 and 3 at fixed end. A state feedback gain for each discrete model of the 3 systems is obtained such that its poles are placed inside the unit circle and has a very good settling time. The individual models of the 3 systems are compared to obtain the best performance.

Comparing the 3 systems, viz., system 1, 2 and 3, it is observed that as the smart beam is divided into 5 finite elements, the vibration characteristics is the best. Hence, it can be concluded that, the best placement of the sensor / actuator pair is at the fixed end of the system 3, i.e., near the root or the hub where the beam is fixed. (the model 1 of system 3). Comparing the responses of the various models of the three systems, system 3's vibration response characteristics are the best for the vibration control of smart beam because of the following reasons.

- A small magnitude of control input u is required to dampen out the vibrations compared to systems 1 & 2.
- The magnitude of the impulse response (open loop and closed loop) of both the continuous and the discrete time system is less compared to systems 1 & 2.
- Also, the response characteristics with F and $\mathbf{L}$ are improved.
- The tip displacements are improved and the vibrations dampen out quickly in this case as seen in table VI.

Responses are simulated for the various models of the plant without control and are compared with the control to show the control effect. It was inferred that without control the transient response was predominant and with control, the vibrations are suppressed. The model 1 of system 3 is more sensitive to the first mode as the bending moment is maximum, strain rate is higher, minimum tip deflection, better sensor output and less requirement of the control input u (control will be more effective), whereas at the free end of the system 3, because of the lesser strain rate and maximum deflection, more control effort is required to damp out the vibrations.

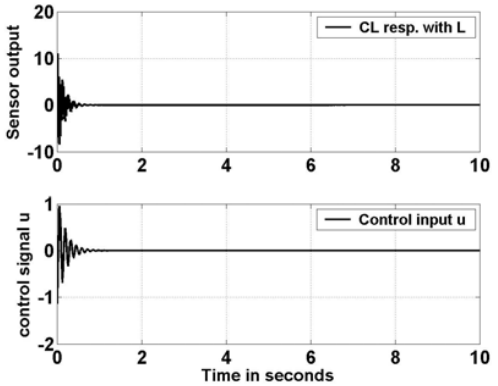

Fig. 6 CL impulse response with FOS feedback gain $\mathbf{L}$ (sensor output y) and control input u, beam divided into 3 finite elements, PZT placed at fixed end

The sensitivity to the higher modes depends not only on the collocation of the piezo pair, but also on many factors such as the gain of the amplifier used, location of the piezo pair at the nodal points , its properties and the number of finite elements. The time responses of the tip displacement w_4, for model 1 of system 1, w_5 (for model 1 of system 2), w_6 (for model 1 of system 3) are also obtained. It was seen that the tip displacement is well controlled and is within limits with the controller.

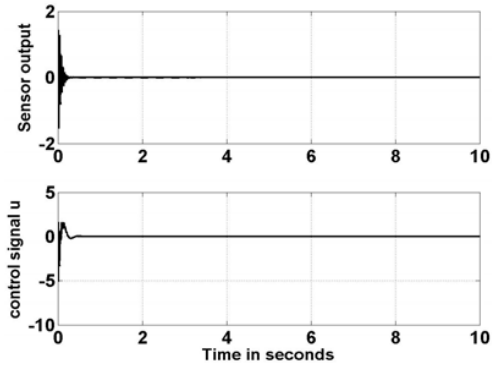

Fig. 7 CL impulse response with FOS feedback gain **L** (sensor output *y*) and control input *u*, beam divided into 3 finite elements, PZT placed at free end

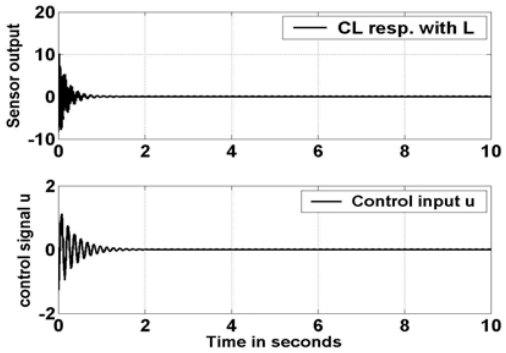

Fig. 8 CL impulse response with FOS feedback gain **L** (sensor output *y*) and control input *u*, beam divided into 4 finite elements, PZT placed at fixed end

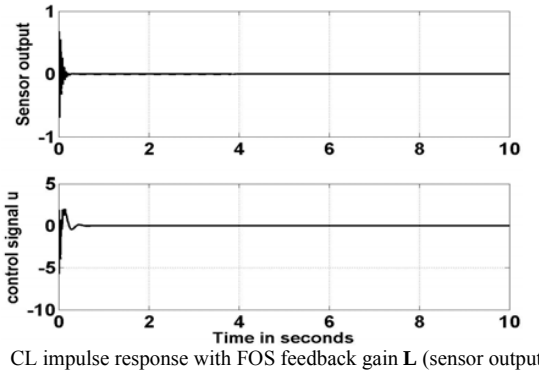

Fig. 9 CL impulse response with FOS feedback gain **L** (sensor output *y*) and control input *u*, beam divided into 4 finite elements, PZT placed at free end

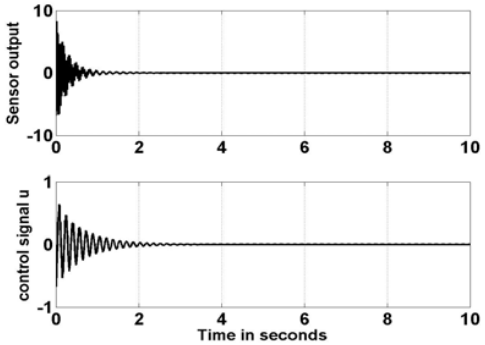

Fig. 10 CL impulse response with FOS feedback gain **L** (sensor output *y*) and control input *u*, beam divided into 5 finite elements, PZT placed at fixed end

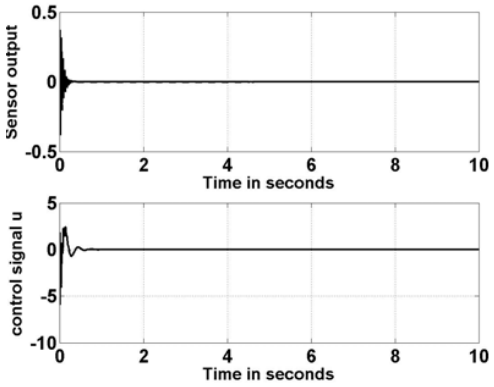

Fig. 11 CL impulse response with FOS feedback gain **L** (sensor output *y*) and control input *u*, beam divided into 5 finite elements, PZT placed at free end

The tip displacements for the models of the Fig. 2 with piezo-patches at fixed end and free end are shown below with the results in table VI.

TABLE VI (a)
TIP DISPLACEMENT SIMULATION RESULTS FOR THE FIXED END

	Fixed end					
	With controller			Without controller		
Model 1, Sys 1	1.8	–1.9	5.3	2.9	–2.7	53
Model 1, Sys 2	0.9	–0.9	4.8	1.3	–1.3	50
Model 1, Sys 3	**0.78**	**–0.6**	**3.8**	0. 8	–0.7	48

TABLE VI (b)
TIP DISPLACEMENT SIMULATION RESULTS FOR THE FREE END

	Free end					
	With controller			Without controller		
Model 3, Sys 1	2.6	–2.6	5.5	2.9	–2.8	25
Model 4, Sys 2	2.1	–2.1	5	2.7	–2.6	22
Model 5, Sys 3	1.5	–1.5	4	2	–1.8	15

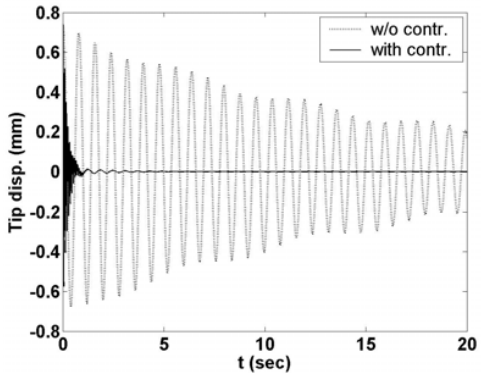

Fig. 12 Tip displacement for model 1 of system 3 (fixed end)

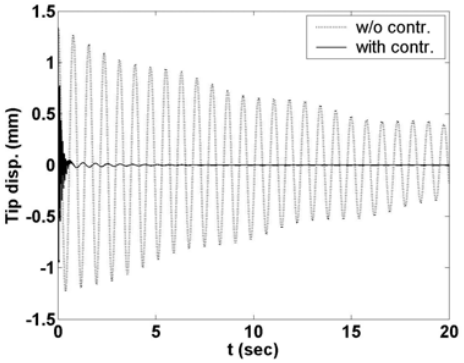

Fig. 13 Tip displacement for model 1 of system 2 (fixed end)

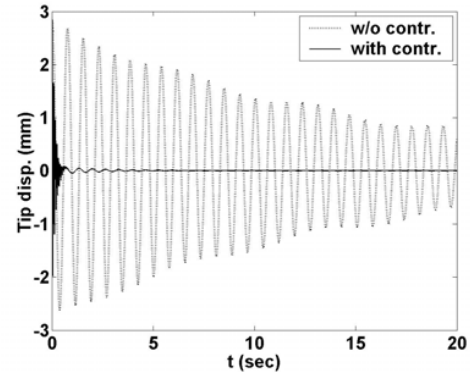

Fig. 14 Tip displacement for model 1 of system 1 (fixed end)

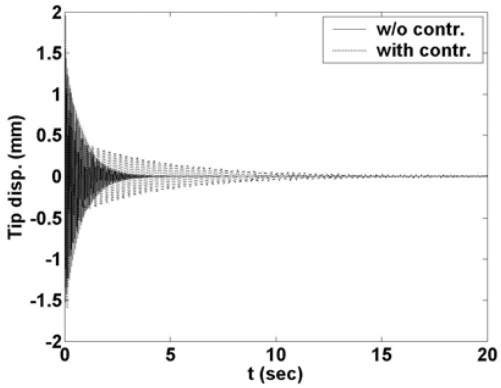

Fig. 15 Tip displacement for model 5 of system 3 (free end)

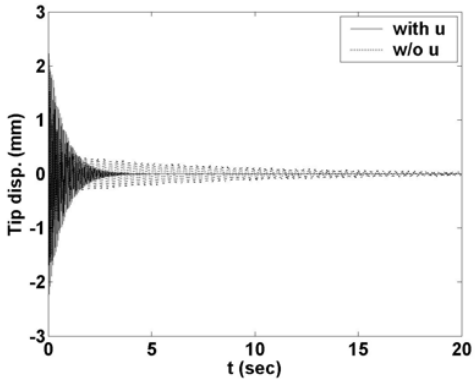

Fig. 16 Tip displacement for model 4 of system 2 (free end)

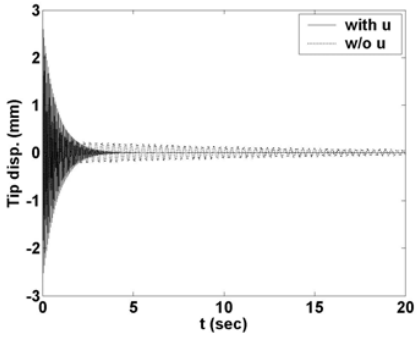

Fig. 17 Tip displacement for model 3 of system 1 (free end)

The frequency response plots (bode plots) of the models of the 3 systems at the fixed end are shown below.

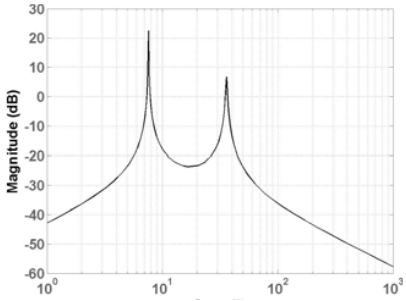

Fig. 18 Bode plots for model 1 of system 1 (fixed end)

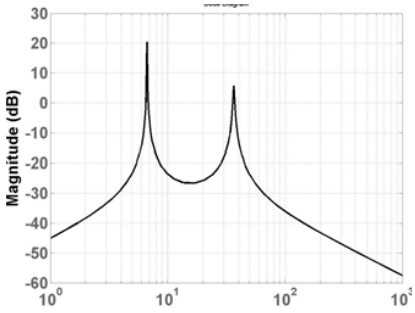

Fig. 19 Bode plots for model 1 of system 2 (fixed end)

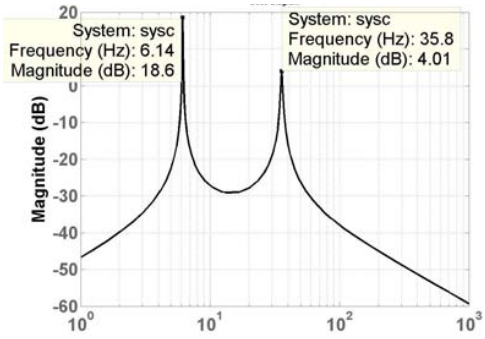

Fig. 20 Bode plots for model 1 of system 3 (fixed end)

ACRONYMS

SISO	Single Input Single Output
FEM	Finite Element Method
PVDF	Poly Vinylidene Derelyne Flouride
FOS	Fast Output Sampling

DOF	Degree Of Freedom
ER	Electro Rheological
MR	Magneto Rheological
AVC	Active Vibration Control
LMI	Linear Matrix Inequalities
PZT	Lead Zirconate Titanate
FE	Finite Element
SS	Smart Structure
CT	Continuous Time
DT	Discrete Time
RHS	Right Hand Side
LTI	Linear Time Invariant
EB	Euler-Bernoulli
PZT	Lead Zirconate Titanate
IOP	Institute of Physics
IEEE	Institute of Electrical and Electronics Engineers
ISSS	Institute of Smart Structures and Systems
SPIE	Society Photonics & Instrumentation Engineers
MATLAB	MATrix LABoratory

NOMENCLATURE (SYMBOLS)

f_{ext}	External force input
l , L	Length of the beam
b	Width of the beam
E_b	Young's modulus of beam
ρ_b	Mass density of beam
α , β	Structural constants
t_b	Thickness of beam
l_p	Length of the piezoelectric patch
t_a	Thickness of actuator
t_s	Thickness of sensor
E_p	Young's modulus of piezoelectric
ρ_p	Mass density of piezoelectric
d_{31}	Piezoelectric strain constant
g_{31}	Piezoelectric stress constant
X, Y, Z	The 3 axis of 3D space
W	Time dependent transverse displacement of Z axis
I	Mass moment of inertia of the beam element
A	Area of cross section of the beam element
T, U	Kinetic energy and strain energy
$\dot{w}$	Linear velocity
δU , δT , δW_e	Variations of the strain energy, the kinetic energy, work done due to the external forces
t	Time in secs
a_i	$(i = 1, 2, 3, 4)$ Unknown coefficients
$\mathbf{q}$	Vector of displacements and slopes
$\dot{\mathbf{q}}$	Strain rate
K^b	Stiffness matrix of the regular beam element (also called as the local stiffness matrix)
M^b	Mass matrix of the regular beam element (also called as the local Mass matrix)
K^p	Stiffness matrix of the piezoelectric element
M^p	Mass matrix of the piezoelectric element
A_p	Area of the piezoelectric patch
E_f	Electric field
D	Dielectric displacement
e	Permittivity of the medium
s^E	Compliance of the medium
d	Piezoelectric constant
$Q(t)$	Charge developed on the sensor surface (due to the strain)
$i(t)$	Current generated by the sensor surface
e_{31}	Piezoelectric stress / charge constant
V^s	Sensor voltage
G_c	Signal-conditioning device gain
K	Controller gain
$\mathbf{p}^T$	Constant vector, which depends on sensor characteristics
$\mathbf{h}^T$	Constant vector, which depends on actuator characteristics
$V^a(t)$	Actuator voltage
$V^s(t)$	Sensor voltage
$\mathbf{f}_{ctrl}$	Control force applied by the actuator
$\mathbf{f}^t$	Total force coefficient vector
$\mathbf{M}$	Assembled mass matrices (global mass matrix)
$\mathbf{K}$	Assembled stiffness matrix (global stiffness matrix)
$\mathbf{T}$	Modal matrix containing the eigenvectors representing the 1st 2 modes
$\mathbf{M}^*$	Generalized mass matrix
$\mathbf{K}^*$	Generalized stiffness matrix
$\mathbf{f}^*_{ext}$ and $\mathbf{f}^*_{ctrl}$	Generalized external force vector and generalized control force vector
$\mathbf{C}^*$	Generalized damping matrix
$\mathbf{g}$	Principal coordinates
$u(t)$	Control input
$r(t)$	External input to the system
$y(t)$	Output of the system, i.e., the sensor output
A, B, C, D	State space matrices (CT) **:** System matrix, input matrix, output matrix, transmission matrix
$\mathbf{E}$	External load matrix which couples the disturbance to the system
$x(t)$	State vector
$\dot{x}(t)$	Derivative of the state vector
$\Re^n$	n dimension space

τ	Sampling interval
Φ_τ, Γ_τ	System matrix, input matrix discritized at sampling interval of τ secs
Φ, Γ	System matrix, input matrix discritized at sampling interval of Δ secs
F	State feedback gain
υ	Observability index of the system
L_j	Output feedback gains
u_k, y_k	Input and output at the k^{th} instant
$\mathbf{C}_0, \mathbf{D}_0$	Lifted system matrices
$\mathbf{L}$	Fast output sampling gain
ρ_1, ρ_2, ρ_3	Spectral norms
I	Identity matrix
N	Number of sub-intervals

REFERENCES

[1] H. Werner and K. Furuta, "Simultaneous stabilization based on output measurements", *Kybernetika*, vol. 31 (4), pp. 395 - 411, 1995.
[2] H. Werner, "Robust control of a laboratory flight simulator by non-dynamic multirate output feedback", *Proc. IEEE Conf. Decision and Control*, pp. 1575-1580, 1996.
[3] E.F. Crawley and J. De. Luis, "Use of piezoelectric actuators as elements of intelligent structures", *AIAA Journal*, vol. 25, pp. 1373 -1385, 1987.
[4] V. L. Syrmos, P. Abdallah, P. Dorato and K. Grigoriadis, "Static output feedback : A survey", *Automatica*, **33(2)**, pp. 125-137, 1997.
[5] P. Gahenet, A. Nemirovski, A.J. Laub and M. Chilali, "LMI Tool Box for Matlab", *The Math works Inc., Natick MA*, 1995.
[6] S. Herman, "Analysis of beams containing piezoelectric sensors and actuators", *Smart Materials Structures Journal*, Vol. 3, pp 439 - 447, 1994.
[7] Woo Seok Hwang and Hyun Chul Park, "Finite Element Modeling of Piezoelectric Sensors and Actuators", *AIAA Journal*, vol. 31 (5), pp. 930-937, 1993.
[8] T. Baily and J. E. Jr. Hubbard, Distributed piezoelectric polymer active vibration control of a cantilever beam", *Journal of Guidance, Dynamics and Control*, vol. 8 (5), pp. 605 - 611, 1985.
[9] P. Seshu, *Textbook of Finite Element Analysis*, 1st ed. Prentice Hall of India New Delhi, 2004.
[10] S. Rao and M. Sunar, "Piezoelectricity and its uses in disturbance sensing and control of flexible structures : A survey," *Applied Mechanics Rev.* vol. 47 (2), pp. 113 – 119, 1994.
[11] B. Culshaw, "Smart structure a concept or a reality," *J. of Syst. Control Engg.* vol. 26 (206), pp. 1-8, 1992.
[12] S. Hanagud and *et al*., "Optimal vibration control by the use of piezoelectric sensors and actuators," *J. of Guid. Control, Dyn.,* vol. 15 (5), pp. 1199 - 1206, 1992.
[13] J. L. Fanson and *et al*., "Positive position feedback control for structures," *AIAA J*., vol. 18 (4), pp. 717 – 723, 1992.
[14] J. Mark Balas "Feedback Control of Flexible Structures," *IEEE Trans. Automat. Contr.*, vol. AC-23 (4), pp. 673-679, 1978.
[15] Herbert Werner, "Multimodal Robust Control by Fast Output Sampling - An LMI Approach," *Automatica*, vol. 34 (12), pp. 1625-1630, 1998.
[16] Sung Kyu Ha, Kailers Ch and Fu Duo Chang, "Finite element analysis of composite structures containing distributed piezoelectric sensors and actuators," *J.* AIAA, vol. 31, pp. 772-780, 1993.
[17] S. B. Choi, C. Cheong and S. Kini., "Control of Flexible Structures by Distributed Piezo-film Actuators and Sensors", *J. of Intelligent Materials and Structures*, vol. 16, 430 – 435, 1995.
[18] A. B. Chammas and C. T. Leondes, "Pole placement by piecewise constant output feedback," *Int. J. Contr.*, vol. 29 (1), pp. 31-38, 1979.
[19] J. S. Burdess and J. N. Fawcett, "Experimental evaluation of piezoelectric actuator for the control of vibrations in a cantilever beam," *J. Syst. Control. Engg.*, vol. 206 (12), pp. 99-106, 1992.
[20] T. D. Fortmann, L. Kleinman and M. Athans, "On the design of linear systems with piecewise constant feedback gains," *IEEE Trans. Auto. Contr.*, vol. AC-13, pp. 345-361, 1968.
[21] W. S. Levine and M. Athans, "On the determine of the optimal constant output feedback gains for linear multivariable systems," *IEEE Trans. Auto. Contr.*, vol. AC-15 (1), pp. 44-48, 1970.
[22] B. Mace, "Active control of flexural vibrations," *J. Sound Vibrn.*, vl. 114 (2), pp. 253-270, 1987.
[23] S.M. Yang and Y. J. Lee, "Optimization of non-collocated sensor / actuator location and feedback gain in control systems," *Smart Materi. Structur.*, vol. 8, pp. 96-102, 1993.
[24] H. Werner and K. Furuta, "Simultaneous stabilization by piecewise constant periodic output feedback," *Control Theory Adv. Technolo.*, vol. 10 (4), pp. 1763-1775, 1995.
[25] Francis Tse, Ivan Morse and Rollnad Hinkle, Mechanical Vibrations-Theory and Applications, *CBS Publishers*, New Delhi, India.